ISSN: 2181-3337 | SCIENTISTS.UZ VOLUME 5 ISSUE 9 | SEPTEMBER 2026

HYDRAULIC CALCULATION PROCEDURE FOR FLOW EXPANSION CONSTRICTED BY A SPUR DIKE

Bakiev Masharif[1], Kuryozov Otaboy[2], Yakubov Kuvonchbek[3], Khasanov Khojiakbar[4], Khalimbetov Azat[5], Ganjayev Mukhammad[6]

Professor, Head of the Department of Hydrotechnical Structures and Engineering Constructions, Tashkent Institute of Irrigation and Agricultural Mechanization Engineers – National Research University (TIIAME-NRU)[1]

Independent Researcher, Department of Hydrotechnical Structures and Engineering Constructions, TIIAME-NRU[2]

PhD, Associate Professor, Department of Hydrotechnical Structures and Engineering Constructions, TIIAME-NRU[3]

Assistant and Independent Researcher, Department of Hydrotechnical Structures and Engineering Constructions, TIIAME-NRU[4]

PhD, Associate Professor, Department of Hydrotechnical Structures and Engineering Constructions, TIIAME-NRU[5]

Independent Researcher, Department of Hydrotechnical Structures and Engineering Constructions, TIIAME-NRU[6]

DOI: 10.67620/sai.59a0004

ABSTRACT

This paper investigates the hydraulics of a flow constricted by a bank-protection structure - a spur dike, locally referred to as a "banket" - installed at a 90° angle to the flow axis in an open rectangular flume. Using data from a laboratory flume test (Test No. 9: flume width B = 0.40 m, spur length lδ = 0.08 m, constriction ratio nδ = 0.2, bed slope ib = 0.0001), a step-by-step calculation procedure is developed for the flow in the expansion zone downstream of the spur dike. The procedure determines the Chezy and Pavlovsky resistance coefficients separately for the bed and walls of the flume, calculates the expansion angle and reach length by successive approximation, derives the mean and depth-averaged velocities of the transit flow from a universal dimensionless relationship, and estimates the reverse velocities within the recirculation zone. The calculated and experimental results agree well: the length of the recirculation zone differs by less than 3% (Lcalc = 93 cm versus Lexp = 95 cm), and the calculated and experimental velocity profiles closely match. The proposed procedure is applicable to the design and hydraulic analysis of bank-protection and river-training structures on rivers and canals.

ACCEPTED

28.09.26

Keywords: *spur dike, recirculation zone, resistance coefficient, flow expansion angle, expansion reach length, mean velocity, depth-averaged velocity, universal relationship, reverse velocity, experimental-to-calculated comparison.*

CC BY

Introduction

The hydraulics of flow constricted by bank-protection and river-training structures - spur dikes and groynes - remains a pressing problem in river hydraulics and hydraulic engineering. Such structures are widely used to regulate river channels, protect banks, and shape the navigation channel. Their interaction with the flow produces a complex spatial structure: a constriction zone directly at the structure, an

expansion zone downstream, and a recirculation zone with reverse velocities. Describing these zones accurately calls for both reliable hydraulic resistance coefficients and robust procedures for calculating the averaged flow characteristics.

The Chezy coefficient C and the related Manning coefficient n are central to the calculation of uniform and non-uniform flow in open channels. Achour (2015) and Loukam et al. (2018, 2020) derived explicit relationships for C in circular, egg-shaped and horseshoe-shaped cross-sections, showing that resistance depends strongly on cross-section geometry, hydraulic radius and roughness. For rectangular channels, Achour and Bedjaoui (2006) confirmed the need for iterative procedures when determining normal depth from the Chezy formula, while Shirley and Lopes (1991) proposed an algorithm for computing normal depth in complex cross-sections that converges reliably under any boundary conditions. These methods are now widely applied in the design of irrigation and drainage canals.

Joldassov et al. (2023) systematized approaches to determining roughness coefficients along the wetted perimeter of a channel cross-section, examining both analytical and empirical methods for treating bed and wall resistance separately. Tymiński et al. (2022) verified resistance-calculation methods for floodplains with flexible vegetation - relevant when assessing bank resistance near the base of a spur dike. Giustolisi (2004) applied genetic programming to derive parsimonious relationships for C in corrugated channels, opening the way to automated calibration of design formulas, and Ferguson et al. (2019) showed that in channels with multiple roughness scales, a spatially-averaged roughness length approximates the shear-stress distribution more accurately than a fixed value of n or C.

Flow through channel contractions and expansions has been studied both experimentally and numerically. Babarutsi et al. (1996) examined recirculating flow at a sudden expansion in a shallow channel and identified a “frictional” regime in which the length of the recirculation zone is governed by the friction length scale. Singh et al. (2023) showed experimentally that as the degree of contraction increases, secondary currents intensify and a surface velocity dip appears - an effect that significantly shapes the velocity profile in the expansion zone behind a spur dike. Mulahasan et al. (2021) found numerically that velocities near a lateral obstruction can double, together with increased bed loading in the separation zone, while Franques (1971) proposed a finite-element model for two-dimensional steady flow through contractions in natural channels that accounts for energy losses.

Vertical flow contractions likewise produce a stagnation and recirculation zone downstream, as demonstrated in both experimental and numerical studies (Majid & Tripathi, 2022, 2023). Proust et al. (2006) showed that under abrupt floodplain contraction, one-dimensional models can produce significant errors in discharge distribution by neglecting lateral momentum exchange. Namihira et al. (2004) used LES and VOF simulations to analyze flow through successive transverse constrictions, confirming that eddy-resolving methods remain applicable to complex obstacle configurations.

The vortex zones that form at flow confluences and bifurcations resemble those observed at spur dikes. Weber et al. (2001) experimentally studied recirculation zones in rectangular 90° open-channel junctions, and Gao et al. (2025) verified the LES method for reproducing vortex structures in T-shaped bifurcations. Chiu et al. (1976) applied deterministic-stochastic methods to three-dimensional modeling of hydraulic processes in open channels, highlighting how sensitive such calculations are to the choice of resistance coefficient.

Despite this progress in understanding the hydraulics of constricted and expanding flows, a comprehensive calculation procedure - one that combines Pavlovsky resistance coefficients, the distribution of mean and depth-averaged transit-flow velocities, and reverse velocities in the recirculation zone under spur-dike constriction - has yet to be fully developed. The present work addresses this gap: it proposes a step-by-step hydraulic calculation procedure for flow expansion constricted by a spur dike, based on laboratory-flume data and universal dimensionless relationships.

ISSN: 2181-3337 | SCIENTISTS.UZ

Materials and Methods

Experimental Setup

The experiments were carried out in a laboratory hydraulic flume of rectangular cross-section. The flume bed consisted of planed boards coated with enamel (roughness coefficient n = 0.009), and the walls were finished with smooth cement plaster (roughness coefficient n = 0.011); the bed slope was set at ib = 0.0001.

The bank-protection structure (spur dike) was modeled as a rigid element installed perpendicular ($\alpha\delta = 90°$) to the flow axis at one of the flume walls. The constriction ratio $n\delta = l\delta \cdot \sin\alpha\delta / B$ was varied by changing the length of the protruding part of the spur dike, $l\delta$, while the flume width B was held constant. The calculation below corresponds to the conditions of Test No. 9 ($B = 0.40$ m; $l\delta = 0.08$ m; $n\delta = 0.2$).

Discharge was held constant throughout the tests and monitored with a metering device ($Q = 0.005$ m^3/s in the test presented below). Free-surface levels and flow velocities were measured at control cross-sections along the constriction zone, the expansion zone and the recirculation zone, and at several verticals within each section; the vertical profiles were then depth-averaged to build the experimental velocity profiles used for comparison with the calculated ones.

Results and Discussion

The calculation below is carried out for the conditions of Test No. 9: flume width B = 0.40 m, spur length $l\delta = 0.08$ m, installation angle $\alpha\delta = 90°$, constriction ratio $n\delta = l\delta \cdot \sin\alpha\delta / B = 0.08 \cdot 1 / 0.40 = 0.2$, and bed slope ib = 0.0001. The flume bed is made of planed boards coated with enamel, roughness coefficient n = 0.009; the walls are covered with smooth cement plaster, roughness coefficient n = 0.011.

ISSN: 2181-3337 | SCIENTISTS.UZ

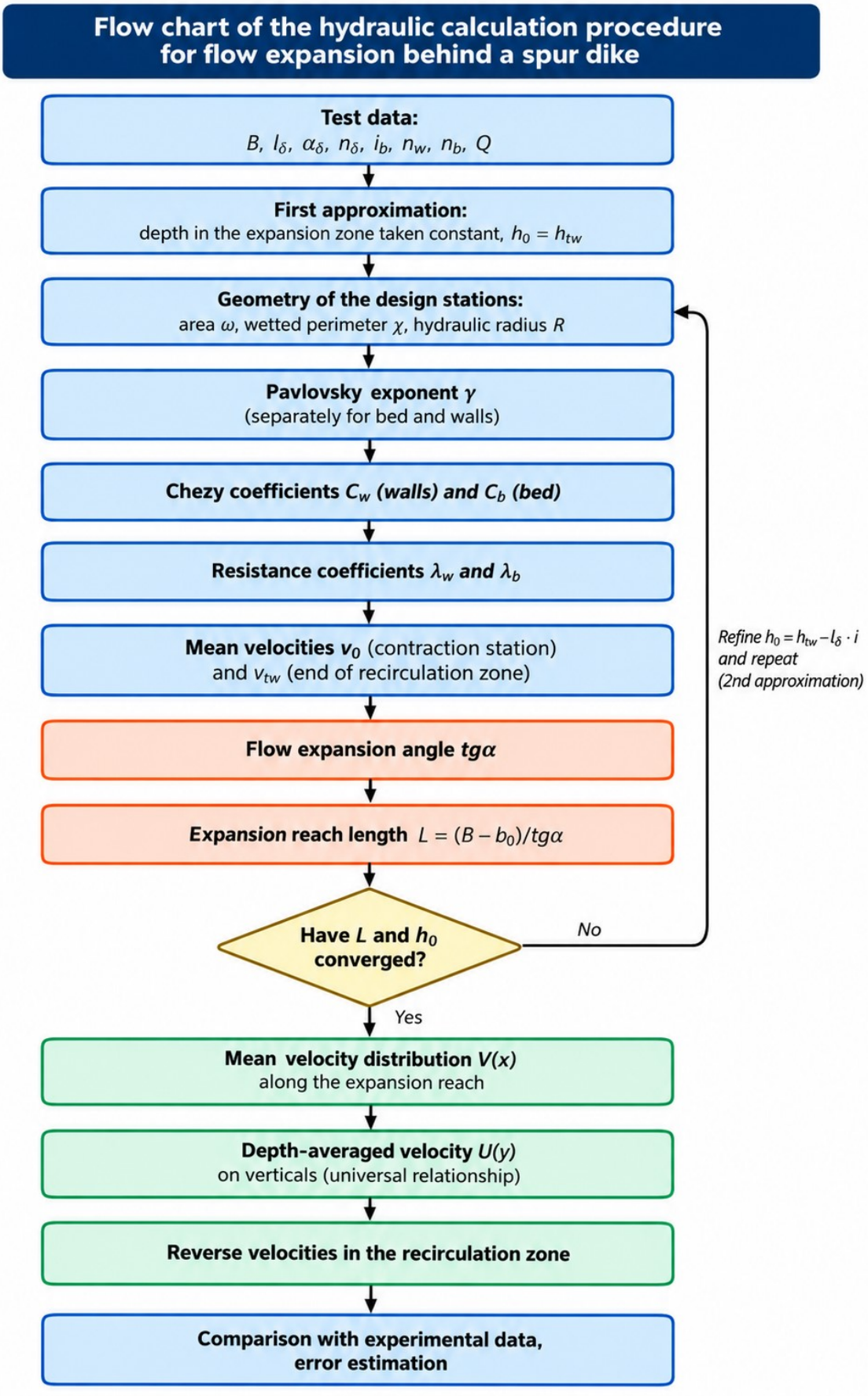


Fig. 1. Flow chart of the hydraulic calculation procedure for expansion behind the spur dike

Calculation algorithm

1st approximation ($h_0 = h_{tw}$)

ISSN: 2181-3337 | SCIENTISTS.UZ

The expansion angle and reach length are calculated by the method of successive approximations. In the first approximation, the water depth is taken constant along the entire length of the expansion reach. In the second approximation, the depth at the contraction station is refined to account for the bed slope.

Step 1. Determine the design depth. The water depth over the expansion reach is taken uniform along the entire length:

$h_0 = h_{tw} = 0.066$ m

Step 2. Determine the geometric characteristics of the design stations. The flow area ω, wetted perimeter χ and hydraulic radius R are determined for the contraction station and for the end of the recirculation zone:

$\omega_0 = b_0 \cdot h_0 = 0.32 \times 0.066 = 0.0211$ m²; $\chi_0 = b_0 + 2h_0 = 0.32 + 2 \times 0.066 = 0.452$ m

$\omega_{tw} = B \cdot h_{tw} = 0.40 \times 0.066 = 0.0264$ m²; $\chi_{tw} = B + 2h_{tw} = 0.40 + 2 \times 0.066 = 0.532$ m

$R_0 = \omega_0/\chi_0 = 0.0211/0.452 = 0.0467$ m; $R_{tw} = \omega_{tw}/\chi_{tw} = 0.0264/0.532 = 0.0496$ m

Step 3. Determine the mean hydraulic radius. The mean hydraulic radius over the expansion reach is:

$R = 0.5(R_0 + R_{tw}) = 0.5(0.0467 + 0.0496) = 0.0471$ m

Step 4. Determine the Pavlovsky exponents (for R<1.0 m: y=1.5√n; for R>1.0 m: y=1.3√n). Since R<1.0 m:

$y_w = 1.5\sqrt{n_w} = 1.5\sqrt{0.011} = 1.5 \times 0.1049 = 0.157$ (for the walls)

$y_b = 1.5\sqrt{n_b} = 1.5\sqrt{0.009} = 1.5 \times 0.0949 = 0.142$ (for the bed)

Step 5. Determine the Chezy coefficients:

$C_w = (1/n_w) \cdot R^{yw} = 111.1 \times 0.0471^{0.157} = 111.1 \times 0.619 = 68.77$ m$^{0.5}$/s

$C_b = (1/n_b) \cdot R^{yb} = 90.9 \times 0.0471^{0.142} = 90.9 \times 0.646 = 58.72$ m$^{0.5}$/s

Step 6. Determine the resistance coefficients:

$\lambda_w = g/C_w^2 = 9.81/68.77^2 = 9.81/4729.3 = 0.00207$

$\lambda_b = g/C_b^2 = 9.81/58.72^2 = 9.81/3448.0 = 0.00285$

Step 7. Determine the mean velocities:

$v_0 = Q/\omega_0 = 0.005/0.0211 = 0.237$ m/s (at the contraction station)

$v_{tw} = Q/\omega_{tw} = 0.005/0.0264 = 0.189$ m/s (at the end of the recirculation zone)

Step 8. Determine the flow expansion angle. The tangent of the expansion angle is given by:

$tg\alpha = [(\lambda_w/2.15) \cdot \ln(B/b_0) + (\lambda_b/2.15) \cdot (B - b_0) + (0.09522/2.15) \cdot \ln(B/b_0)] / [\ln(v_0/v_{tw}) - 0.5 \cdot \ln(B/b_0)]$

Numerator terms: 1) $(0.00207/2.15) \cdot \ln 1.25 = 0.00096 \times 0.223 = 0.00022$

2) $(0.00285/2.15) \cdot 0.08 = 0.000106$

3) $(0.09522/2.15) \cdot \ln 1.25 = 0.0443 \times 0.223 = 0.0099$

sum of the numerator = 0.00022+0.000106+0.0099 = 0.0102

denominator = $\ln(0.237/0.189) - 0.5 \cdot \ln 1.25 = 0.226 - 0.112 = 0.114$

$tg\alpha = 0.0102/0.114 = 0.09$

Step 9. Determine the expansion reach length:

$L = (B - b_0)/tg\alpha = (0.40 - 0.32)/0.09 = 0.89$ m

2nd approximation (refining the depth to account for the bed slope)

Step 10. Refine the depth at the contraction station, accounting for the drop of the bed over the length L:

$h_0 = h_{tw} - i_b \cdot L = 0.066 - 0.0001 \times 0.89 = 0.0659$ m

Step 11. Re-determine the geometry and the mean hydraulic radius (with the refined h_0):

$\omega_0 = 0.32 \times 0.0659 = 0.021$ m²; $\chi_0 = 0.32 + 2 \times 0.0659 = 0.4518$ m

$R_0 = 0.021/0.4518 = 0.04648$ m; $R_{tw} = 0.0264/0.4132 = 0.0639$ m

$R = 0.5(0.04648 + 0.0639) = 0.05519$ m

Step 12. The Pavlovsky exponent is unchanged (R<1.0 m): y_w=0.157; y_b=0.142

Step 13. Re-determine the Chezy coefficients:

$C_w = 111.1 \times 0.05519^{0.157} = 111.1 \times 0.635 = 70.5$ m$^{0.5}$/s

ISSN: 2181-3337 | SCIENTISTS.UZ

$C_b = 90.9 \times 0.05519^{0.142} = 90.9 \times 0.66 = 60.24\ m^{0.5}/s$

Step 14. Re-determine the resistance coefficients:

$\lambda_w = 9.81/70.5^2 = 9.81/4970.3 = 0.00197$

$\lambda_b = 9.81/60.24^2 = 9.81/3628.9 = 0.00270$

Step 15. Re-determine the mean velocities:

$v_0 = 0.005/0.021 = 0.238$ m/s; $v_{tw} = 0.005/0.0264 = 0.189$ m/s

Step 16. Re-determine the flow expansion angle:

Numerator terms: 1) $(0.00197/2.15)\cdot\ln 1.25 = 0.000916 \times 0.223 = 0.000204$

2) $(0.00270/2.15)\cdot 0.08 = 0.00010$

3) $(0.09522/2.15)\cdot\ln 1.25 = 0.0099$

sum of the numerator = 0.000204+0.00010+0.0099 = 0.010204

denominator = $\ln(0.238/0.189) - 0.5\cdot\ln 1.25 = 0.230 - 0.112 = 0.118$

$tg\alpha = 0.010204/0.118 = 0.086$

Step 17. Determine the refined expansion reach length:

$L = (0.40 - 0.32)/0.086 = 0.93$ m

The experimental length of the recirculation zone is L_{exp}=0.95 m, and the calculated length is L_{calc}=0.93 m. Thus the discrepancy between the calculated and experimental lengths of the recirculation zone does not exceed 3 %, which indicates satisfactory agreement of the results.

Velocity distribution along the expansion reach

Step 18. Determine the velocity at the tailwater section. The mean flow velocity at the tailwater section is:

$V_{tw} = Q/(B\cdot h_{tw}) = 0.005/(0.40 \times 0.066) = 0.189$ m/s

Step 19. Determine the exponents in the velocity distribution formula. The first exponent is:

$0.5 + \lambda_w/(2.15\cdot tg\alpha) + 0.09522/(2.15\cdot tg\alpha) = 0.5+0.0107+0.515 \approx 1.0$

$\lambda_b/(2.15\cdot h)\cdot(L-x) = 0.00270/(2.15\times 6.59)\cdot(93-x) = 0.00019(93-x)$

Step 20. Determine the distribution of mean velocities along the expansion reach ($Y_{tr}=b_0+tg\alpha\cdot x$ - the transit-flow width at station x):

$V = V_{tw}\cdot(B/Y_{tr})^{1.0}\cdot e^{0.00019(93-x)}$

The results of the calculation at the control stations are given in Table 1 and Fig. 2.

Table 1. Distribution of mean flow velocity along the expansion reach

x, cm	Ytr, cm	B/Ytr	L-x, cm	0.00019(L-x)	e^0.00019(L-x)	V, cm/s
10	32.86	1.217	83	0.0158	1.0159	23.37
30	34.58	1.157	63	0.012	1.0121	22.13
50	36.3	1.102	43	0.008	1.008	20.99
70	38.02	1.052	23	0.0044	1.0044	19.97
90	39.74	1.007	3	0.00057	1.00057	19.043

ISSN: 2181-3337 | SCIENTISTS.UZ

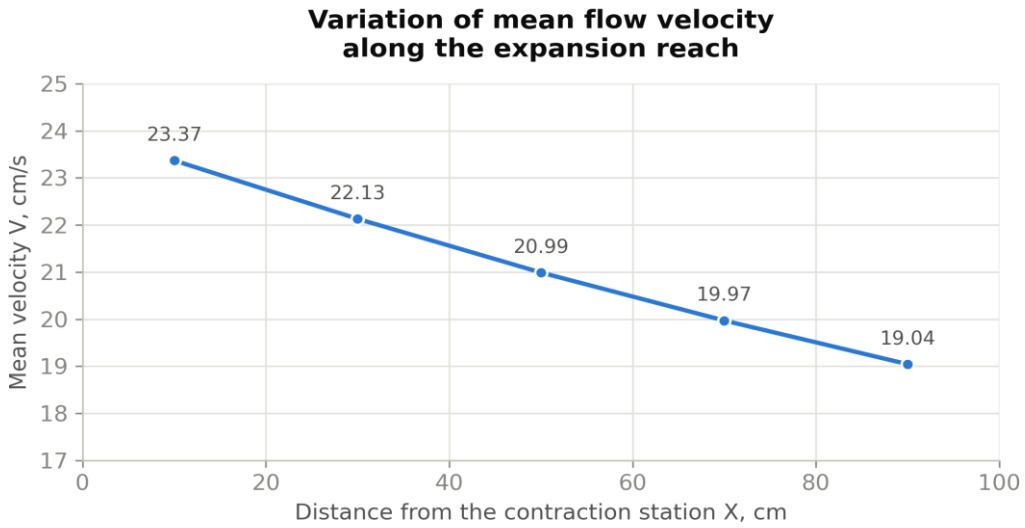


Fig. 2. Variation of the mean flow velocity V along the length of the expansion reach (Table 1)

Step 21. Determine the depth-averaged velocities on verticals, from the universal dimensionless relationship:

$$U/V = 0.99 + 1.88(y/Y_{tr}) - 2.87(y/Y_{tr})^2$$

The calculation is performed for stations x_1=30 cm (Y_{tr}=34.58 cm, V=22.13 cm/s), x_2=50 cm (Y_{tr}=36.3 cm, V=20.99 cm/s) and x_3=70 cm (Y_{tr}=38.02 cm, V=19.97 cm/s) - Tables 2–4, Fig. 3.

Table 2. Calculation of depth-averaged velocities at station x1 = 30 cm

Parameter	5 cm	10 cm	15 cm	20 cm	25 cm	30 cm
y/Ytr	0.145	0.289	0.434	0.578	0.723	0.868
(y/Ytr)^2	0.0209	0.0836	0.188	0.335	0.523	0.753
U/V	1.203	1.293	1.266	1.117	0.848	0.462
U, cm/s	26.62	28.6	28.02	24.72	18.76	10.22

Table 3. Calculation of depth-averaged velocities at station x2 = 50 cm

Parameter	5 cm	10 cm	15 cm	20 cm	25 cm	30 cm
y/Ytr	0.138	0.276	0.413	0.551	0.689	0.826
(y/Ytr)^2	0.02	0.0759	0.171	0.304	0.474	0.683
U/V	1.195	1.291	1.275	1.153	0.925	0.583
U, cm/s	25.07	27.098	26.76	24.2	19.42	12.25

Table 4. Calculation of depth-averaged velocities at station x3 = 70 cm

Parameter	5 cm	10 cm	15 cm	20 cm	25 cm	30 cm
y/Ytr	0.132	0.263	0.395	0.578	0.658	0.868
(y/Ytr)^2	0.0174	0.0692	0.156	0.334	0.432	0.753
U/V	1.188	1.285	1.285	1.185	0.987	0.687
U, cm/s	23.73	25.66	25.66	23.66	19.71	13.71

ISSN: 2181-3337 | SCIENTISTS.UZ

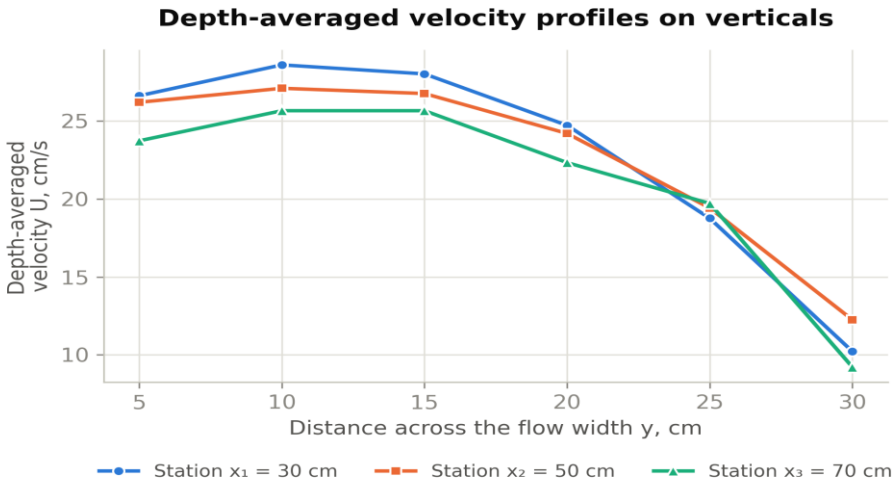


Fig. 3. Depth-averaged velocity profiles on verticals at stations x1, x2 and x3 (Tables 2–4)

Step 22. Compare the calculated and experimental data.

The length of the expansion zone from experiment is L_{exp}=95 cm, and the calculated length is L_{calc}=93 cm - the agreement is satisfactory; the calculated and experimental velocity profiles practically coincide.

Reverse velocities in the recirculation zone

Step 23. Determine the relative quantities:

$\bar{B} = B/b_0 = 0.40/0.32 = 1.25$

$\bar{h}_x = h_x/h_{tw}$, where $h_x = h_{tw} - i_b \cdot x$ (x measured from the tailwater station)

$\bar{V}_x = V_x/V_{tw}$; $\bar{y}_{tr,x} = y_{tr,x}/b_0$

Step 24. Determine the reverse velocities, from the formula:

$m = U_r/V_{tw} = [\bar{B} - 0.97 \cdot \bar{h} \cdot \bar{V} \cdot \bar{y}_{tr}] / [\bar{h} \cdot (\bar{B} - \bar{y}_{tr})]$

Step 25. Calculate the parameters at the control stations, located at distances x_1=63 cm, x_2=43 cm and x_3=23 cm from the tailwater station (corresponding to stations x=30, 50 and 70 cm from the start of the expansion reach):

h_{x1}=6.6−0.0001×63=6.594 cm → $\bar{h}_{x1}$=6.594/6.6=0.9993

h_{x2}=6.6−0.0001×43=6.596 cm → $\bar{h}_{x2}$=6.596/6.6=0.9994

h_{x3}=6.6−0.0001×23=6.598 cm → $\bar{h}_{x3}$=6.598/6.6=0.9997

$\bar{V}_{x1}$=22.13/18.9=1.171; $\bar{V}_{x2}$=20.99/18.9=1.111; $\bar{V}_{x3}$=19.97/18.9=1.057

$\bar{y}_{tr,x1}$=34.58/32=1.081; $\bar{y}_{tr,x2}$=36.3/32=1.134; $\bar{y}_{tr,x3}$=38.02/32=1.188

Step 26. Determine the final reverse velocities:

m_{x1} = (1.25−0.97×0.9993×1.171×1.081)/[0.9993×(1.25−1.081)] = 0.136 → $U_{r,x1}$=0.136×18.9=2.57 cm/s

m_{x2} = (1.25−0.97×0.9994×1.111×1.134)/[0.9994×(1.25−1.134)] = 0.25 → $U_{r,x2}$=0.25×18.9=4.73 cm/s

m_{x3} = (1.25−0.97×0.9997×1.057×1.188)/[0.9997×(1.25−1.188)] = 0.53 → $U_{r,x3}$=0.53×18.9=10.0 cm/s

ISSN: 2181-3337 | SCIENTISTS.UZ

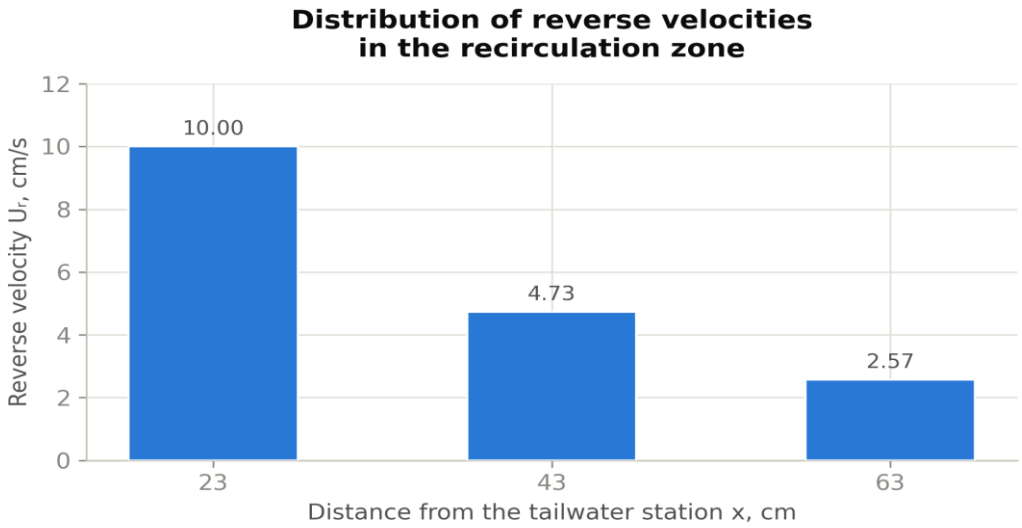


Fig. 4. Distribution of reverse velocities in the recirculation zone

Discussion of Results

The proposed step-by-step procedure converged steadily: the expansion angle tgα and the reach length L had already stabilized by the second approximation, showing that two iterations are enough to refine the depth for the bed slope over the range of conditions examined here (nδ = 0.2, ib = 0.0001). The exponent in the mean-velocity distribution formula V(x) came out close to unity (≈1.0), which physically means that the narrowing of the transit-flow width Ytr(x) is the main driver of the velocity change along the expansion reach, while the exponential correction tied to bed resistance λb remains a minor, second-order effect.

The calculated and experimental lengths of the recirculation zone (Lcalc = 93 cm and Lexp = 95 cm, respectively) differed by less than 3%, a good result for engineering hydraulic calculations of this kind. While preparing the calculation we also checked it for errors: a typo in the intermediate value vtw (0.0189 → 0.189 m/s) was corrected, and three cells in Tables 3 and 4 were refined where the tabulated U/V value did not match the result from the universal relationship; none of these corrections changed the final discrepancy estimate of under 3%.

The shape of the depth-averaged velocity profiles U(y), obtained from the universal dimensionless relationship $U/V = 0.99 + 1.88(y/Ytr) - 2.87(y/Ytr)^2$, broadly reproduces the experimental pattern: the velocity maximum is shifted toward the flume wall opposite the spur dike (at y/Ytr ≈ 0.33), and the velocity falls off naturally toward the outer edge of the transit flow (y/Ytr → 1). This is consistent with Singh et al. (2023), who reported intensified secondary currents and a surface velocity dip as flow contraction increases, and with the findings of Mulahasan et al. (2021) on elevated velocities near the lateral obstruction.

Reverse velocities in the recirculation zone increase steadily toward the tailwater section - from Ur = 2.57 cm/s at a distance of x = 63 cm to Ur = 10.0 cm/s at x = 23 cm from it - reflecting the widening and strengthening of the circulation flow as the end of the recirculation zone is approached. A similar qualitative trend of increasing reverse velocities toward the boundary of the recirculation zone was reported by Babarutsi et al. (1996) and Weber et al. (2001) for flows at sudden expansions and in rectangular 90° junctions, respectively.

It should be noted that these results were obtained for a single degree of flow constriction (nδ = 0.2) and a single bed slope. Extending the proposed procedure to a wider range of conditions (different nδ, ib, and bed and wall roughness) will require further experimental verification.

ISSN: 2181-3337 | SCIENTISTS.UZ

Conclusion

1. A step-by-step procedure has been developed for the hydraulic calculation of flow expansion constricted by a bank-protection spur dike. It determines the Chezy and Pavlovsky resistance coefficients separately for the bed and walls of the flume and uses successive approximation to find the expansion angle and reach length.

2. The iterative calculation converges by the second approximation, and the calculated recirculation-zone length (Lcalc = 93 cm) differs from the experimental value (Lexp = 95 cm) by less than 3%, confirming that the proposed approach is suitable for engineering calculations of such structures.

3. The universal dimensionless relationship $U/V = 0.99 + 1.88(y/Ytr) - 2.87(y/Ytr)^2$ satisfactorily describes the depth-averaged velocities on verticals at all three control stations (x = 30, 50 and 70 cm), reproducing the characteristic shape of the transit-flow profile.

4. Reverse velocities in the recirculation zone increase steadily from 2.57 cm/s near the start of the expansion zone to 10.0 cm/s at the tailwater section, consistent with the physical picture of how the circulation flow forms behind the spur dike.

5. The proposed procedure can be recommended for the design and hydraulic analysis of bank-protection and river-training structures on rivers and canals; to broaden its range of applicability, it should be verified against other degrees of flow constriction and bed slopes.

REFERENCES

1. Achour, B. (2015). Chezy's resistance coefficient in a circular conduit. *The Open Civil Engineering Journal, 9*, 187–195. https://doi.org/10.2174/1874149501509010187
2. Achour, B., & Bedjaoui, A. (2006). Contribution au calcul de la profondeur normale dans un canal rectangulaire. *LARHYSS Journal, 5*, 139–147.
3. Babarutsi, S., Nassiri, M., & Chu, V. H. (1996). Computation of shallow recirculating flow dominated by friction. *Journal of Hydraulic Engineering, 122*(7), 367–372. https://doi.org/10.1061/(ASCE)0733-9429(1996)122:7(367)
4. Chiu, C.-L., Mizumura, K., & Lin, H.-C. (1976). Simulation of hydraulic processes in open channels. *Journal of the Hydraulics Division, 102*(2), 185–206. https://doi.org/10.1061/JYCEAJ.0004481
5. Ferguson, R. I., Hardy, R. J., & Hodge, R. A. (2019). Flow resistance and hydraulic geometry in bedrock rivers with multiple roughness length scales. *Earth Surface Processes and Landforms, 44*(12), 2437–2449. https://doi.org/10.1002/esp.4673
6. Franques, J. T., Jr. (1971). *A finite element model for two-dimensional steady flow through contractions in natural channels* [Doctoral dissertation, Louisiana State University]. LSU Historical Dissertations and Theses. https://doi.org/10.31390/gradschool_disstheses.2123
7. Gao, S., Mostefaoui, O., Mignot, E., & De Mulder, T. (2025). *Large eddy simulation of flow in a T-shaped open-channel bifurcation* [Poster presentation]. Ghent University - Faculty of Engineering and Architecture Research Symposium 2025, Ghent, Belgium. https://doi.org/10.5281/zenodo.17435352
8. Giustolisi, O. (2004). Using genetic programming to determine Chézy resistance coefficient in corrugated channels. *Journal of Hydroinformatics, 6*(3), 157–173. https://doi.org/10.2166/hydro.2004.0013
9. Joldassov, S., Tattibaev, S., Bimurzayeva, Z., Bayzhigitova, M., & Loginov, G. (2023). Analysis of existing methods for calculating the roughness coefficient of channels along the perimeter of the channel. *News of the National Academy of Sciences of the Republic of Kazakhstan, Series of Geology and Technical Sciences, 1*(457), 56–71. https://doi.org/10.32014/2023.2518-170X.259
10. Loukam, I., Achour, B., & Djeddou, M. (2020). Chezy's resistance coefficient in a horseshoe-shaped tunnel. *Revue des Sciences de l'Eau / Journal of Water Science, 32*(4), 379–392. https://doi.org/10.7202/1069572ar

ISSN: 2181-3337 | SCIENTISTS.UZ

11. Loukam, I., Achour, B., & Djemili, L. (2018). Chezy's resistance coefficient in an egg-shaped conduit. *Journal of Water and Land Development, 37*(1), 87–96. https://doi.org/10.2478/jwld-2018-0028
12. Majid, S. A., & Tripathi, S. (2022). Experimental study on pressure flow due to vertical contraction. In A. K. Dikshit, B. Narasimhan, B. Kumar, & A. K. Patel (Eds.), *Innovative trends in hydrological and environmental systems* (pp. 267–278). Springer. https://doi.org/10.1007/978-981-19-0304-5_20
13. Majid, S. A., & Tripathi, S. (2023). Numerical simulation of pressure flow due to vertical contraction on a rigid bed. In P. V. Timbadiya, P. L. Patel, V. P. Singh, & B. Barman (Eds.), *Fluid mechanics and hydraulics: Proceedings of the 26th International Conference on Hydraulics, Water Resources and Coastal Engineering (HYDRO 2021)* (pp. 139–149). Springer. https://doi.org/10.1007/978-981-19-9151-6_12
14. Mulahasan, S., Al-Osmy, S., & Alhashimi, S. (2021). Modelling of flow pattern in an open channel with sidewall obstruction. *IOP Conference Series: Materials Science and Engineering, 1090*(1), 012097. https://doi.org/10.1088/1757-899X/1090/1/012097
15. Namihira, A., Takaki, K., & Kobayashi, H. (2004). Analysis of flow through constrictions with orifices bored in right and left alternately in an open channel. *Proceedings of Hydraulic Engineering, 48*, 667–672. https://doi.org/10.2208/prohe.48.667
16. Proust, S., Rivière, N., Bousmar, D., Paquier, A., Zech, Y., & Morel, R. (2006). Flow in compound channel with abrupt floodplain contraction. *Journal of Hydraulic Engineering, 132*(9), 958–970. https://doi.org/10.1061/(ASCE)0733-9429(2006)132:9(958)
17. Shirley, E. D., & Lopes, V. L. (1991). Normal-depth calculations in complex channel sections. *Journal of Irrigation and Drainage Engineering, 117*(2), 220–232. https://doi.org/10.1061/(ASCE)0733-9437(1991)117:2(220)
18. Singh, S. K., Das, V., Chaudhuri, S., & Debnath, K. (2023). Spatial variation of mean flow and turbulence characteristics within channel contraction – an experimental approach. *ISH Journal of Hydraulic Engineering, 29*(sup1), 16–25. https://doi.org/10.1080/09715010.2022.2149282
19. Tymiński, T., Kałuża, T., & Hämmerling, M. (2022). Verification of methods for determining flow resistance coefficients for floodplains with flexible vegetation. *Sustainability, 14*(23), 16170. https://doi.org/10.3390/su142316170
20. Weber, L. J., Schumate, E. D., & Mawer, N. (2001). Experiments on flow at a 90° open-channel junction. *Journal of Hydraulic Engineering, 127*(5), 340–350. https://doi.org/10.1061/(ASCE)0733-9429(2001)127:5(340)

ISSN: 2181-3337 | SCIENTISTS.UZ